Available online at www.sciencedirect.com
ScienceDirect
Journal of Power Sources 174 (2007) 206–220
JOURNAL OF POWER SOURCES
www.elsevier.com/locate/jpowsour

Physical degradation of membrane electrode assemblies undergoing freeze/thaw cycling: Micro-structure effects

S. Kim [a,b], M.M. Mench [a,*]

[a] *Fuel Cell Dynamics and Diagnostics Laboratory, Department of Mechanical and Nuclear Engineering, The Pennsylvania State University, University Park, PA 16802, United States*
[b] *Research & Development Division, Hyundai Motor Company, Yongin 446-912, Republic of Korea*

Received 3 July 2007; received in revised form 18 August 2007; accepted 30 August 2007
Available online 11 September 2007

Abstract

The objective of this work is to investigate physical damage of polymer electrolyte fuel cell (PEFC) materials subjected to freeze/thaw cycling. Effects of membrane electrode assembly micro-structures (catalyst layer cracking, membrane thickness, and membrane reinforcement) and diffusion media with micro-porous layers were analyzed by comparing scanning electron microscopy images of freeze/thaw cycled samples (−40 °C/70 °C) with those of virgin material and thermal cycled samples without freezing (5 °C/70 °C). Ex situ testing performed in this study has revealed a strong direction for the material choices in the PEFC and confirmed the previous computational model in the literature [S. He, M.M. Mench, J. Electrochem. Soc., 153 (2006) A1724–A1731; S. He, S.H. Kim, M.M. Mench, J. Electrochem. Soc., in press]. Specifically, the membrane electrode assemblies were found to be a source of water that can damage the catalyst layers under freeze/thaw conditions. Damage was found to occur almost exclusively under the channel, and not under the land (the graphite that touches the diffusion media). Conceptually, the best material to mitigate freeze-damage is a crack free virgin catalyst layer on a reinforced membrane that is as thin as possible, protected by a stiff diffusion media.

Keywords: Polymer electrolyte fuel cell; Degradation; Freeze/thaw; Frost heave; Membrane

1. Introduction

Hydrogen fuel cells are the most promising power source for the next generation of vehicles due to their high power density, rapid dynamic response, and relatively benign emissions. However, for fuel cell vehicles to be commercially viable, there are several barriers to be overcome, including: durability, cost, cold start ability, and hydrogen storage and delivery infrastructure. Issues related to subfreezing operation, including rapid start-up, energy consumption, survivability, and durability have recently become the subjects of investigation. For fuel cell vehicles to be competitive, they should deliver 90% of rated power in 30 s from a cold start at −20 °C, with less than 62.5 J/W_e parasitic energy input [3]. Moreover, fuel cells should survive without damage after repeated soaking at −40 °C. Cold start and survivability issues are attributed to the existence of residual liquid water after shutdown, or water generation during the cold start-up.

This paper is concerned with residual liquid water from shutdown. When fuel cells are exposed to a subfreezing ambient atmosphere, ice is formed. Expansion and contraction due to the ice formation and melting process, and the frost heave process caused by capillary forces [1,2] can cause mechanical stress or delamination in the fuel cell materials, leading to material degradation. On start-up, existence of ice or ice formation can also delay start-up time and require external energy input. Redistribution and the amount of residual water in fuel cell materials during the shutdown play an important role in elucidating the damage mode. In the Nafion® membrane, three kinds of water phases, free water, freezable loosely bounded water, and non-freezable water exist. Non-freezable water is highly polarized in hydration shells and is unable to crystallize. Free water behaves like bulk water which exhibits sharp a freezing peak in differential scanning calorimetry (DSC) at 0 °C. Freezable weakly bounded water interacts weakly with ion cores, which displays relatively broad freezing depression

* Corresponding author. Tel.: +1 814 865 0060; fax: +1 814 863 4848.
E-mail address: mmm124@psu.edu (M.M. Mench).

0378-7753/$ – see front matter © 2007 Elsevier B.V. All rights reserved.
doi:10.1016/j.jpowsour.2007.08.111

Table 1
Summary of observed PEFC damage due to freezing

Reference	Test mode	Membrane	CL	MEA	DM	Test conditions			Results	Publication
						T range (°C)	Number of cycles	Purge/no purge		
Wilson et al. [15]	In situ F/T	Nafion® 117	20 wt.% Pt/C (0.16 mg cm^{-2})	Decal process [a]	ELAT hydrophobic carbon cloth	−10/80	3	No purge (wet)	No performance loss	1994
McDonald et al. [7]	Ex situ F/T	Nafion® 112	0.4 mg Pt/C cm^{-2}	N/A	None	−40/80	385	Dry state ($\lambda < 3$)	No remarkable physical damage; change in the molecular level	2004
	In situ F/T	Nafion® 112	0.4 mg Pt/C cm^{-2}	N/A	Carbon paper		385	Dry state ($\lambda < 3$)	No remarkable physical damage; change in the molecular level	
Liu [18]	Ex situ F/T (immersion)	Nafion® 112	N/A	N/A	None	−40/50	10	Immersed in water	Severe CL loss; severe deformation of MEA	2006
		DSM	N/A	N/A	None		10	Immersed in water	No observable loss	
	In situ F/T	Nafion® 112	N/A	N/A	N/A		40	N/A	No performance loss; no ECSA loss	
		DSM	N/A	N/A	N/A		40	N/A	No performance loss; no ECSA loss	
Patterson et al. [19,20]	In situ F/T	N/A	N/A	N/A	N/A	−40/25	63	N/A	No performance loss	2006
	Cold start-up	N/A	N/A	N/A	N/A	−15	N/A	N/A	End cell loss	
Mukundan et al. [16,17]	In situ F/T	Nafion® 1135	20 wt.% Pt/C (0.2 mg cm^{-2})	Decal process[a]	Wet proofed carbon cloth	−40/80	100	No purge (wet)	No performance loss	2006
					SGL 30 DC[b]		45	No purge (wet)	Mechanical failure of GDL	
		Nafion® 1135	20 wt.% Pt/C (0.2 mg cm^{-2})		Wet proofed carbon cloth	−80/80	10	No purge (wet)	Performance loss; HFR increase; interfacial delamination GDL failure	
Cho et al. [10,11]	In situ F/T	Nafion® 115	20 wt.% Pt/C (0.4 mg cm^{-2})	GDE[c]	Wet proofed carbon paper	−10/80	4	No purge (wet)	Performance loss, ohmic and charge transfer resistance increase; ECSA loss	2003
							4	Dry purge ($\lambda < 2$)	No performance loss; no ECSA loss	2004
Gaylord [12]	Field test (stationary)	N/A	N/A	N/A	Carbon paper	Exposed to freezing	N/A	N/A	DM fracture; membrane failure; severe CL delamination	2005
Meyers [13]	In situ F/T	Commercial MEAs (reinforced membrane)			N/A	−20/NA	20	N/A	Membrane cracks; CL delamination	2005
Oszcipok et al. [21,22]	Cold start-up	Catalyst coated membrane			N/A	−10	10	Dry purge	Performance loss; ECSA loss; Hydrophobicity loss (MPL, DM)	2005
		Catalyst coated membrane (0.4 mgPt cm^{-2})			Carbon cloth	−10	7	Partial purge	Significant performance loss	2006
Yan et al. [14]	Cold start-up	Nafion® 112,115,117	20 wt.% Pt/C	GDE[d]	Carbon paper/cloth	−15	NA	N/A	Interfacial delamination; membrane hole	2006
Guo et al. [8]	Ex situ F/T	Commercial MEA with 30 μm membrane and 1.0 mg Pt cm^{-2}	None		6	Dry purge ($\lambda < 4$)	Negligible damage			
				−30/20				2006		
			No purge (wet)	Severe damage; severe CL cracks						
	In situ F/T		Carbon paper	20	No purge (wet)		Severe CL cracks; ECSA loss; negligible performance loss; easy flooding			
					Dry purge ($\lambda < 4$)		No physical damage; no performance loss			
Hou et al. [9]	In situ F/T	Nafion® 212	20 wt.% Pt/C (0.8 mgPt cm^{-2})	GDE[e]	Carbon paper	−20/60	20	Dry purge ($\lambda < 2$)	No performance loss; no ECSA loss; no physical damage	2006

Abbreviations: F/T, freeze/thaw thermal cycling; DSM, dimensionally stable membrane; GDE, gas diffusion electrode; MEM, membrane.

[a] Decal printing (TBA + form catalyst) and then hot pressing at 200 °C.

[b] 20% PTFE treatment with MPL.

[c] Catalyst ink sprayed on DM and then hot pressing at 140 °C.

[d] Sprayed on DM and then hot pressed.

[e] Sprayed on DM.

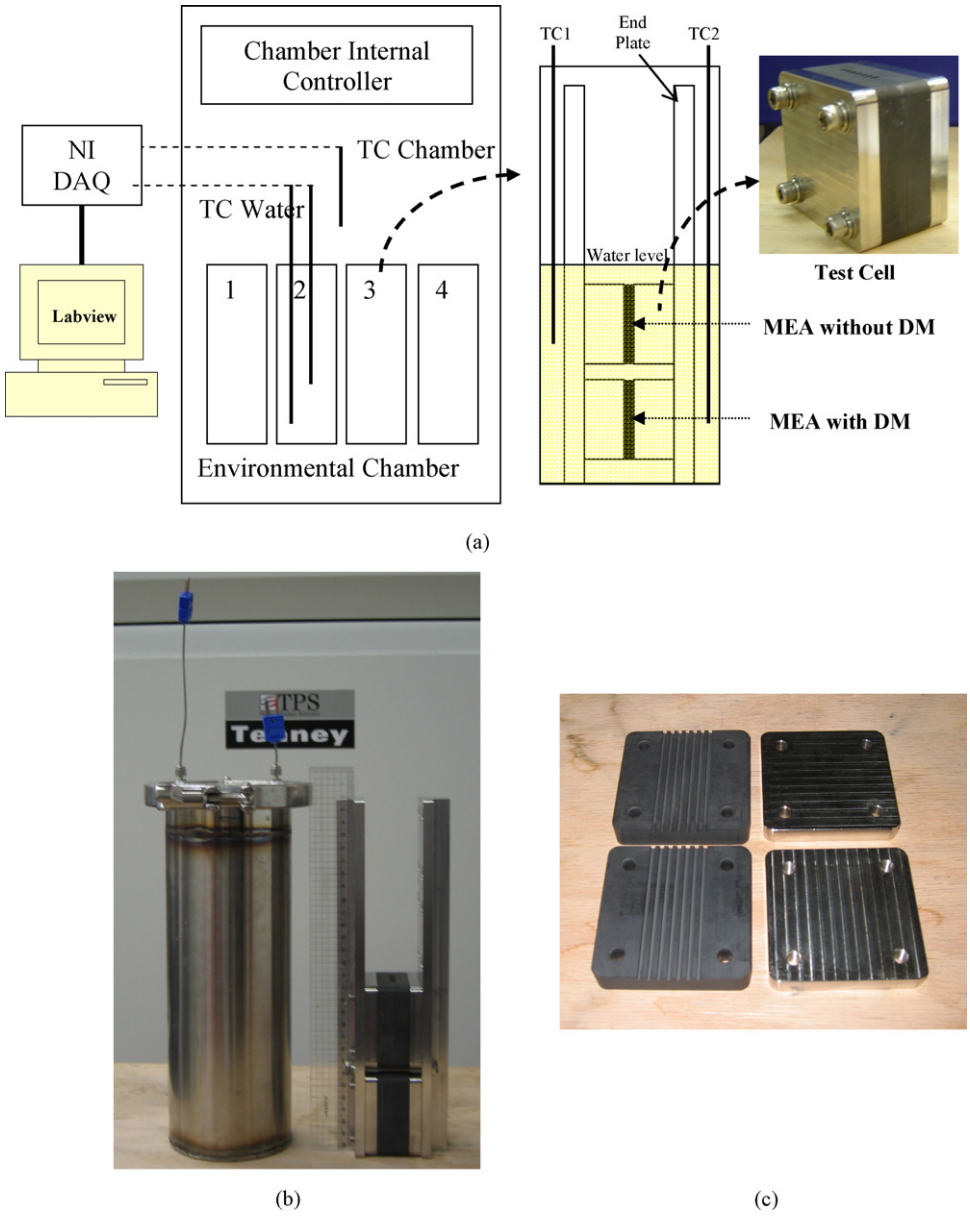

Fig. 1. Schematic and pictures of test setup used for the ex situ freeze/thaw thermal cycling tests. (a) Schematic of test setup, (b) vessel and assembled test cells, and (c) flow field plate and compression plate.

below −20 °C [4–6]. The water content among the three phases ($\lambda = H_2O/SO_3^-$) in the Nafion® membrane is reported differently [4–6]: 17–20.8 (total), 2.2–13.1 (non-freezable water), 8.3–13.1 (weakly bounded water), and 0–4.9 (free water). Freezable water (weakly bounded and free water) redistributes during the shutdown and is a key factor for freeze/thaw (F/T) cycling damage by ice lens formation [1,2]. However, water phase and transport behaviors under freezing conditions are not yet completely understood.

Existing findings on damage by freezing are summarized chronologically in Table 1. One important result shows that fuel cells dried during the shutdown experience neither observable physical damage nor electrochemical losses by freezing [7–10]. However, there are conflicting results in case of a cell with no significant purge. Some reported physical damage, performance loss, and electrochemical loss (electrochemical catalytic surface area (ECSA), interfacial and charge transfer resistance increase) [8,11–14]. Physical damage includes membrane failure (holes and cracks) [12–14], catalyst cracks and delamination [8,13], pore distribution change [11], and gas diffusion media fracture [12]. Others observed no significant performance loss even without dry purge during the shutdown [15–17]. UTC Fuel Cells observed severe damage owing to freezing, but with stack design changes, damage is reported to be prevented [13,19,20].

Liu [18] investigated the effects of membrane reinforcement and diffusion media on freezing damage. Contrary to a non-reinforced membrane electrode assembly (MEA) with a dimensionally stable reinforced membrane had no observable damage in the ex situ immersion F/T thermal cycling test, which indi-

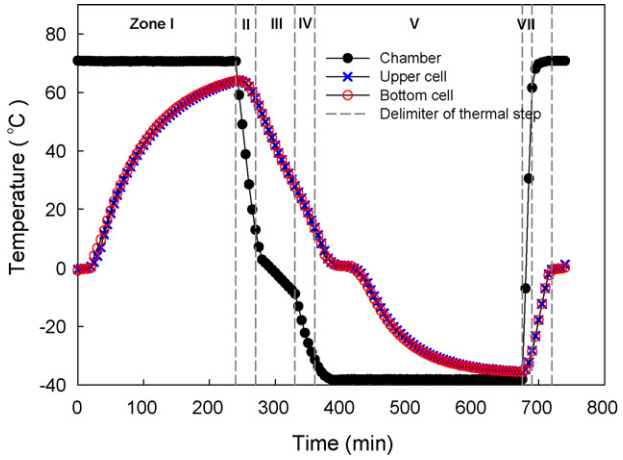

Fig. 2. Thermal freeze/thaw cycling profile of the environmental chamber and the water of the upper cell (TC 1) and the lower cell (TC 2) inside the test vessel.

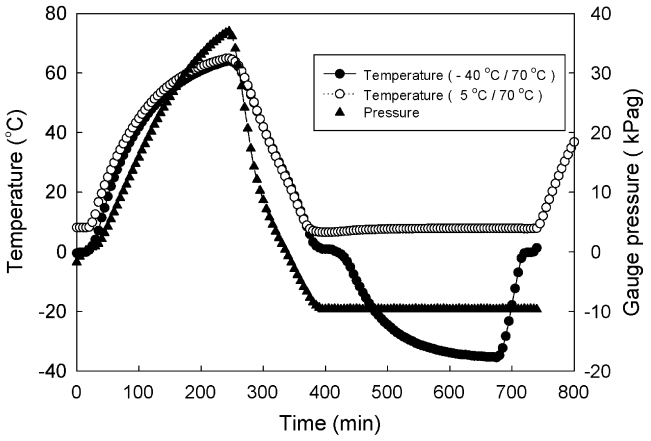

Fig. 3. Temperature and pressure profile of water inside the vessel between 70 °C/5 °C cycling and 70 °C/−40 °C cycling.

cated a reinforced membrane is more tolerable to F/T damage. Interestingly, both MEAs with diffusion media (DM) had no observable damage. This indicates diffusion media can be an important factor to mitigate F/T damage.

Literature on damage during the cold start tests is rare, but performance loss, ECSA loss and hydrophobicity loss was observed [21,22] and end cell loss, especially anode end cell, was reported [19,20]. Compared to thermal freeze/thaw cycling, more severe damage during the cold start may be expected because of fast ice formation.

The F/T damage may be a coupled effect of MEA and DM materials because the residual water content in each can behave as a source of water. Hydrophobic treatment in the DM and micro-porous layer (MPL) can serve as a barrier for direct water flow from water outside the MEA structure, and as mechanical support for the catalyst layer (CL). Therefore, effects of DM and MEAs on damage need to be separated to understand the possible damage modes.

The F/T damage is affected by several factors including MEA manufacturing processes, micro-structures, and CL compositions. Decal processes using tetrabutylammonium (TBA) form of ionomers make a much stronger bonding between CL and ionomers compared to an ink spraying method. Direct coating on a membrane with TBA form catalyst ink can create a more intimate membrane/electrode interface compared to a decal process [15]. Some conflicting results about freeze-damage may be ascribed to different manufacturing processes. Physical damage can also be aggravated in the case of weakly bonded CL to ionomers or membrane. Therefore, micro-structure, composition, and manufacturing process of MEAs are also important factors on F/T damage.

Damage can also be due to stress induced by volume expansion at phase transformation. However, fuel cell materials are highly porous (70–85% for DM and 40% for CL). Therefore, the 9% of volume expansion from ice formation can be absorbed by porous structure without damage unless nearly fully saturated, providing formation is slow. Simple stress effects induced by ice formation are not sufficient to explain interfacial delamination damage mode. He and Mench [1,2] suggested the most possible damage location by ice lens formation are the interfaces between DM, CL, membrane, and flow field plate under the flow channel.

The conflicting claims as to whether freeze/thaw cycling or cold start causes damage can only be resolved with increased understanding and more controlled experimentation. Furthermore, fundamental understanding of the damage and the controlling factors is needed. The objective of this study was to observe fuel cell material damage under the worst-case conditions of liquid water submersion to identify the key factors leading to physical damage. Among several factors, the effects of MEA micro-structures and micro-porous layer coated diffusion media (DM/MPL) were investigated under freeze/thaw cycling conditions in conditions of water immersion.

Table 2
Thickness and crack density of MEAs used

MEA	Thickness (μm)				Virgin crack density (% by area)
	Membrane		CL		
	Reinforced part	Non-reinforced part	Anode	Cathode	
Non-cracked CL with 18 μm reinforced membrane	5–6	10–12	10–13	10–13	0
Cracked CL with 18 μm reinforced membrane	5–6	10–12	10–13	10–13	6–6.8
Non-cracked CL with 35 μm reinforced membrane	8–10	20–25	10–13	10–13	0
Non-cracked CL with 18 μm non-reinforced membrane	0	15–19	10–13	10–13	0

2. Method of approach

2.1. Material testing

Fig. 1 shows a schematic of the ex situ test setup consisting of four test vessels, an environmental chamber (Thermal Product Solutions, Model: T10S-1.5), and a National Instruments Labview™ based data acquisition system. The test vessels were thermally cycled and controlled by an integrated programmable temperature controller with an operating temperature range from −40 °C to 200 °C. A test cell consisted of two graphite flow field plates with seven channels (2 mm width and depth) and two stainless steel compression plates. Test samples were sandwiched by graphite plates and stainless steel compression plates, and compressed by bolts and spring lock washers by the same pressure forces as a normal fuel cell, which was verified by pressure paper. The test cells were assembled with additional stainless steel end plates in order to have similar temperature boundary conditions. Two identical MEAs were tested in the same vessel, where the upper test cell was assembled with a MEA without DM/MPL and the second lower cell with a MEA with DM/MPL. Two additional DM/MPL materials were inserted between the upper test cell and end plate to maintain uniform compression and similar temperature boundary conditions.

The thermal profile of the environmental chamber was calibrated, and Fig. 2 shows the measured thermal profile of the test bath and chamber. The thermal profile used for cycling was set to the following by the internal programmable unit:

(I) soaking at 70 °C for 4 h 30 min;
(II) cooling from 70 °C to 5 °C for 30 min;
(III) cooling from 5 °C to −10 °C for 1 h;
(IV) cooling from −10 °C to −40 °C for 30 min;
(V) soaking at −40 °C for 5 h 15 min;
(VI) heating from −40 °C to 70 °C for 15 min.

As shown in Fig. 2, temperature profiles of the upper cell and the lower cell are almost the same, so that comparison between two test cells is valid. To identify damage induced by only freeze/thaw cycling, additional thermal cycling without freezing between 5 °C and 70 °C was also performed. To make heat transfer rates of two cases (without freezing/with freezing) similar, the chamber temperature profile was calibrated. From Fig. 3, it is clear that temperature profile during the heat up and cooling down of both cases are almost the same, so legitimate comparison is possible, and the potential heat transfer rate effect on liquid transport is not a factor in these tests.

Four MEA types, supplied by W.L. Gore and Associates, were tested to investigate effects of membrane thickness, reinforcement of membrane, and virgin CL crack density. The four MEA types consisted of (1) virgin non-cracked CL with 18 μm reinforced membrane, (2) virgin cracked CL with 18 μm reinforced membrane, (3) virgin non-cracked CL with 18 μm non-reinforced membrane, and (4) virgin non-cracked CL with 35 μm reinforced membrane. The composition and manufacturing processes of the CL of all four MEAs were identical, and the Pt loading in the anode and cathode CL respectively was 0.4 mg cm^{-2}. Micro-structures and compositions of anode and cathode were also identical, which enabled us to eliminate compositional and manufacturing effects on F/T damage. All four types of MEAs experienced 30 thermal cycles with freezing (−40 °C to 70 °C) and without freezing (5–70 °C). To investigate effects of DM/MPL on F/T damage, a paper DM/MPL, SGL 10BB (SGL Carbon Group, USA) was used.

The MEAs without DM were directly in contact with liquid water, the worst possible case. However, in case of the MEAs with DM/MPL, SGL 10BB blocks direct contact of liquid water with MEA if external pressure is not applied to overcome capillary pressure. Pressurizing the test vessels is required to ensure the MEA humidified. In this ex situ test, water vapor pressure increase as a result of temperature change during the F/T cycling was utilized, as shown in Fig. 3. The pressure of the sealed test vessel increases with temperature, because of water saturation vapor and ideal gas effects. The pressure was measured by a pressure transducer (Omega Engineering Inc., Model: PX209-30V15GI, gauge pressure range: −100 kPag to 100 kPag). The gauge pressure reaches 37.92 kPag at the maximum temperature and as cooling proceeds, the pressure decreases to −8.96 kPag. Even when the pressure profile is repeated, water saturation inside the porous media should not change with time, because the negligible hydrostatic pressure difference across the porous material fully immersed in the water cannot transport water out of the porous media. Based on experimental capillary pressure versus saturation level of SGL10BB, the liquid water saturation level is estimated to be about 50% in these conditions [25]. Therefore, water level in the thermally cycled MEA with DM/MPL (SGL10BB) is above fully vapor saturated. This test condition is less severe than MEA without DM/MPL (with 100% liquid contact), but is anticipated to be more severe than actual fuel cell situations, allowing us to observe the key factors in physical damage under F/T conditions.

The thickness and surface crack density of tested MEAs are summarized in Table 2. The surface crack area density of virgin cracked MEA was measured by using ImageJ [26] software. It should be noted that cracks did not include internal voids observed occasionally in the membrane/catalyst layer interfaces, and were a result of the manufacturing process. Five scanning electron microscopy (SEM) images (magnification 50×) were used to assess the average crack density.

2.2. Sample preparation for SEM image

Tested samples were stored in a sealed zipper bag to maintain the same humidity level. To observe morphologies by SEM, tested samples were exposed to ambient atmosphere to dry out for at least 8 h. Surface morphologies of thermally cycled MEAs without DM/MPL were observed using a sample holder template. The template had the same size as test samples, and consisted of three windows across the channel to observe uniformity of damage. To observe the cross-sectional image of cycled

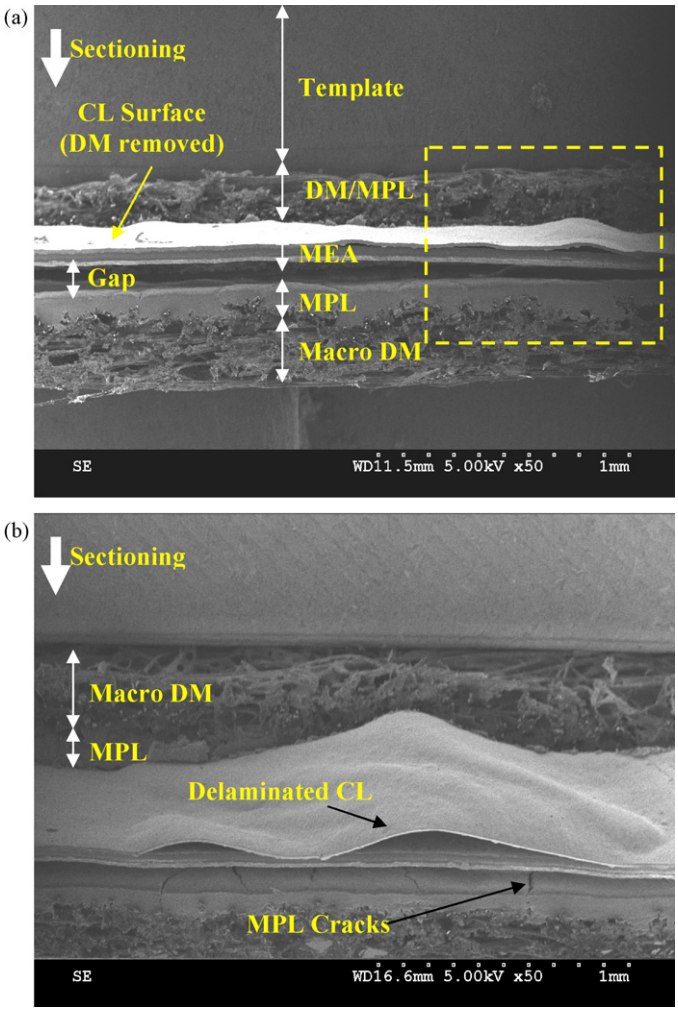

Fig. 4. Typical cross-sectional and magnified images of CL surface of cycled MEA with DM/MPL: (a) cross-sectional image and (b) magnified image of the dotted box of (a).

MEAs without DM/MPL, sectioning of samples was prepared by applying a new razor blade vertically on the cycled sample across the channel direction. The sectioned MEA was assembled between aluminum templates having the same channel and land geometry.

To observe surface and cross-sectional images of cycled MEAs with DM/MPL, the DM/MPL must be removed without damage. The cycled DM/MPL-attached MEA was cut across the channel. Then the DM/MPL sample was cut from the surface side intended for observation, enabling the DM/MPL to be removed with negligible damage. By cutting with a new razor blade on the removed sliced MEA surface, sectional samples were prepared. The cutting direction is important, because the sectioning itself may cause delamination. The membrane/electrode interface under the membrane (bottom part) may be delaminated, but delamination of the interface of the top part should be negligible. Figures in this work are shown as cut from top to bottom. A typical sectioned image is shown in Fig 4. Surface images of cycled MEA with DM/MPL were observed by rotating and tilting the same cross-sectional sample. A close-up image of DM/MPL-removed surface (denoted as a dotted rectangle) is shown in the bottom of Fig. 4. The gap between MEA and DM/MPL was ascribed to uneven compression of sample holder, not to F/T damage. Surface morphologies and cross-sectional images of virgin, F/T cycled, and thermally cycled but not frozen materials were observed.

3. Results

Fig. 5 shows surface SEM images of virgin MEAs with cracked (6.0–6.8% by area) and non-cracked catalyst layers. It also shows sectional SEM images of virgin MEAs with reinforced membrane [27] and non-reinforced membrane. It should also be noted that membrane was exposed inside the cracks, which can serve as water pooling sites.

3.1. Thermal cycling effects of MEAs without DM

Fig. 6 shows images of the non-cracked CL with 18 μm reinforced membrane. On the top row of images, no damage was observed in the condition subjected to thermal cycling without freeze between 5 °C and 70 °C. However, separation of catalyst layers was observed under the channel when thermally cycling with freezing from −40 °C to 70 °C. No such damage was observed under the land, due to the high compression force applied, which restricts ice lens growth and expansion damage. A cross-sectional view of the damage for this configuration is given in Fig. 7, showing the catalyst layer separation exclusively under the channel location for the frozen condition.

Figs. 8 and 9 show surface and cross-sectional SEM images of a thermally cycled initially cracked CL with 18 μm reinforced membrane without DM/MPL. Similar to the non-cracked MEA, the damage was observed under the channels. Due to the initial cracking, however, it appears the resultant damage after freeze/thaw cycling was more severe. It was also observed that simple thermal cycling without freeze did not induce morphological damage. The membrane in the initially cracked MEA, of which the membrane between the cracks was exposed to water, was not apparently damaged by F/T cycling.

Figs. 10 and 11 show surface and cross-sectional SEM images of a thermally cycled initially non-cracked CL with 35 μm reinforced membrane without DM/MPL. Interestingly, the damage for this MEA was much more severe than for the similar non-cracked 18 μm reinforced case, indicating the thickness of the MEA does play a role in the damage process, as predicted by the modeling results [1]. Nearly, complete delamination of the catalyst layer under the channels was seen. Again, the non-frozen samples do not show any obvious morphological damage, although a thin crack along the channel/land interface was seen. We determined from other results that this was prevented with use of the diffusion media.

Figs. 12 and 13 show surface and cross-sectional SEM images of a thermally cycled initially non-cracked CL with 18 μm non-reinforced membrane without DM/MPL. The damage for this non-reinforced membrane case was much more severe than for

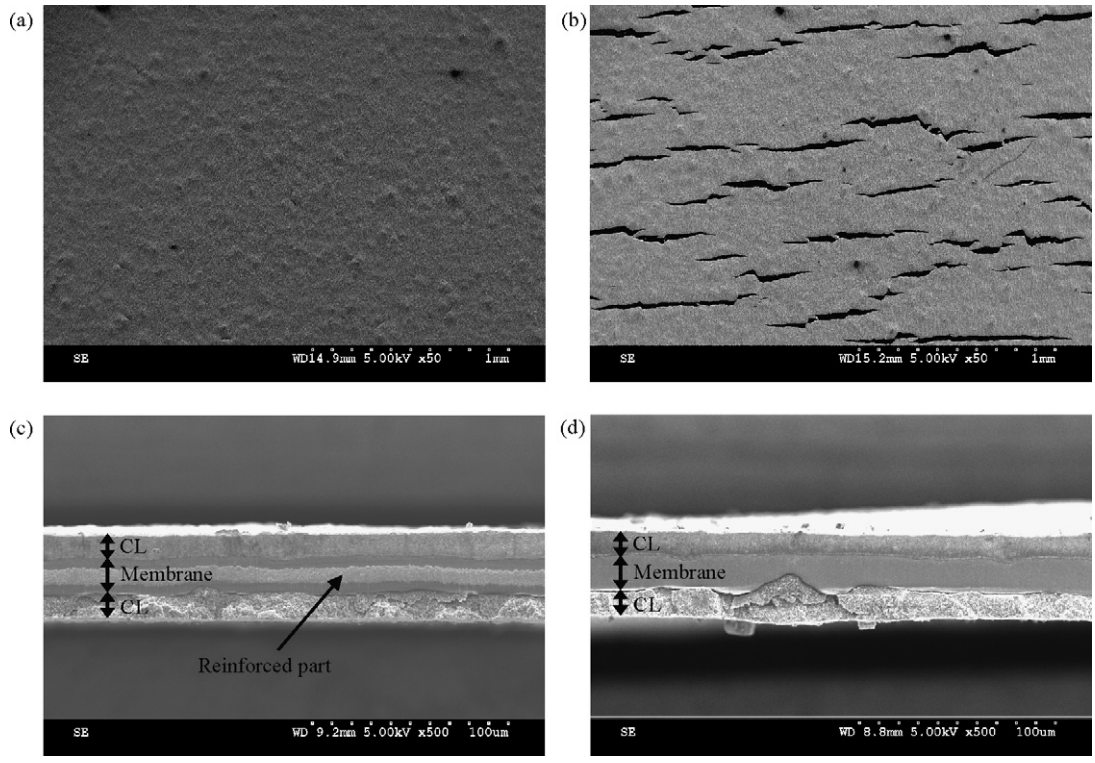

Fig. 5. SEM surface and sectional images of virgin MEA samples used in testing. (a) Non-cracked catalyst layers, (b) initially cracked catalyst layers, (c) MEA with reinforced membrane, and (d) MEA with non-reinforced membrane.

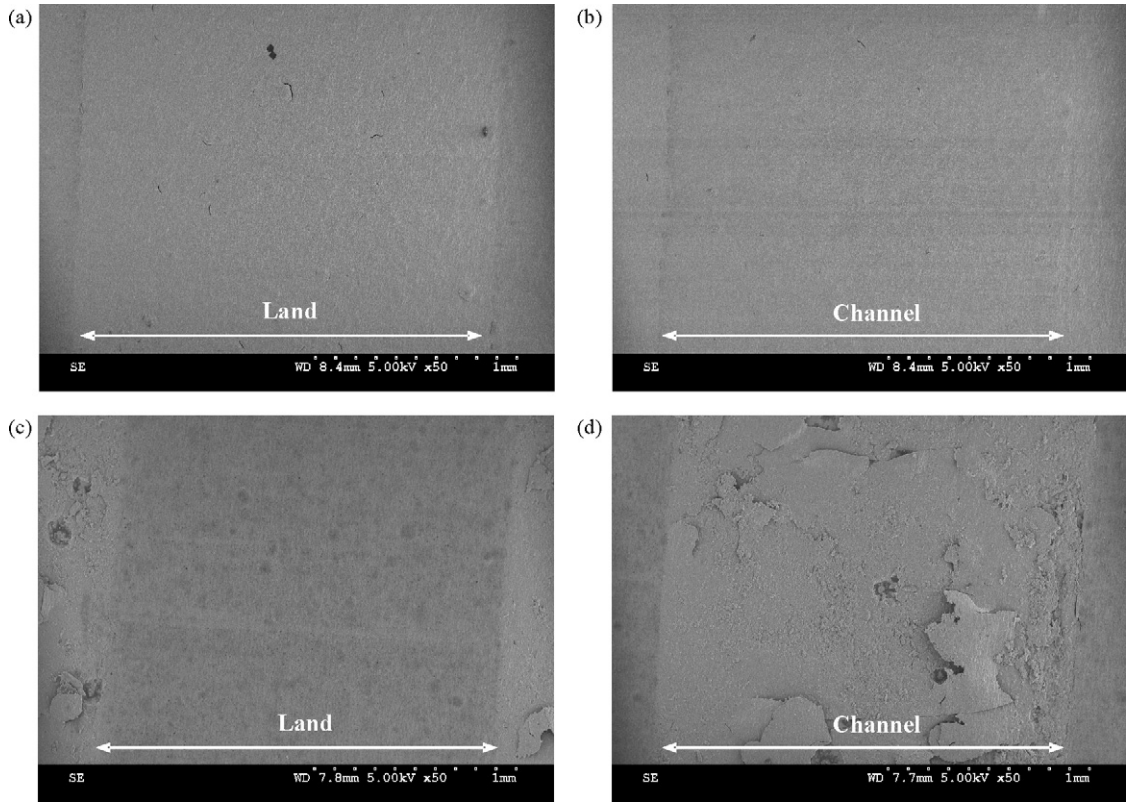

Fig. 6. SEM surface images of thermally cycled non-cracked CL with 18 μm reinforced membrane without DM: (a) land, 5 °C/70 °C, (b) channel, 5 °C/70 °C, (c) land, −40 °C/70 °C, and (d) channel, −40 °C/70 °C.

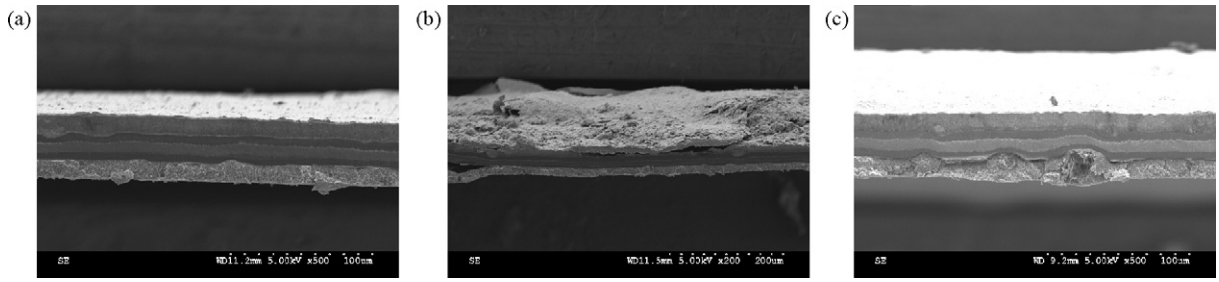

Fig. 7. Cross-sectional images of thermally cycled non-cracked CL with 18 μm reinforced membrane without DM: (a) −40 °C/70 °C, land, 500×, (b) −40 °C/70 °C, channel, 200× and (c) 5 °C/70 °C, channel, 500×.

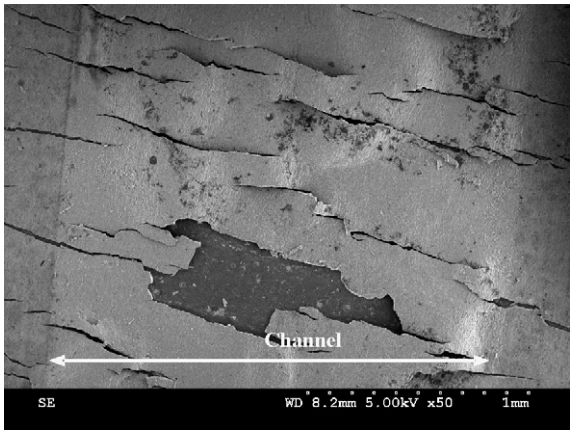

Fig. 8. SEM surface images of F/T cycled initially cracked CL with 18 μm reinforced membrane without DM located under the channel.

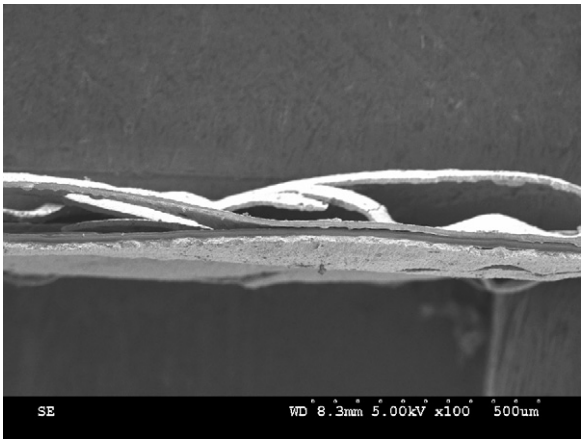

Fig. 9. Sectional image of F/T cycled initially cracked CL with 18 μm reinforced membrane without DM located under the channel.

the similar case with a reinforced membrane. The extent of damage is similar to the non-cracked 35 μm reinforced case. Nearly complete delamination of CL under the channels was observed. Similar to non-cracked CL with 35 μm reinforced membrane without DM/MPL, a slight line crack along the channel/land interface was observed in the non-frozen MEA that is eliminated with a DM.

3.2. Thermal cycling effects with DM/MPL

Fig. 14 shows cross-sectional SEM images of a thermally cycled initially non-cracked CL with 18 μm reinforced membrane with DM/MPL. The results from cycle testing indicate that this configuration (thin, reinforced, with DM/MPL, without virgin cracks) is the most tolerant to freeze-damage. Unlike the case of the same MEA without DM (shown in Figs. 6 and 7), the surface morphology of CL under the channel was not significantly changed in this case. Some minor cracking under the channels was observed in the frozen case, but it is unclear if this is a result of sectioning, manufacturing, or freeze/thaw. Some isolated locations of CL bubbling can be seen, but they are sporadic and the MEA remained largely intact. The common trend of negligible under-the-land physically observable damage was detected. Thermal cycling without freeze did not cause any

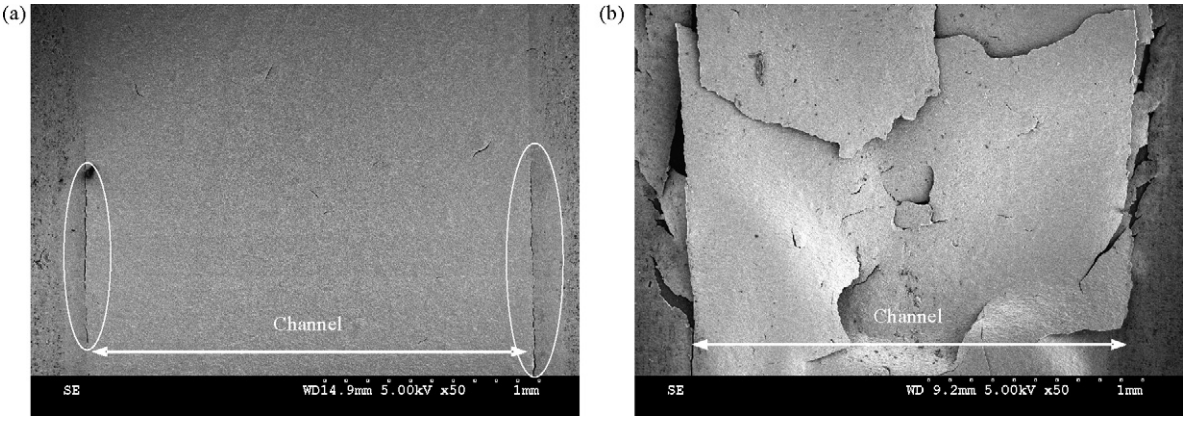

Fig. 10. SEM surface images of non-cracked CL with 35 μm reinforced membrane under the channel locations without DM: (a) 5 °C/70 °C and (b) −40 °C/70 °C.

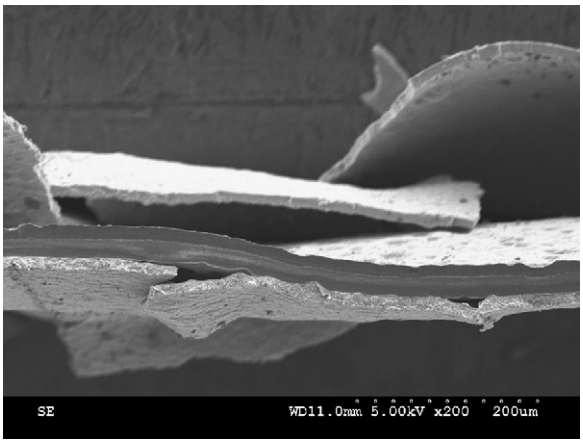

Fig. 11. Cross-sectional images of F/T cycled initially cracked CL with 35 μm reinforced membrane without DM located under the channel.

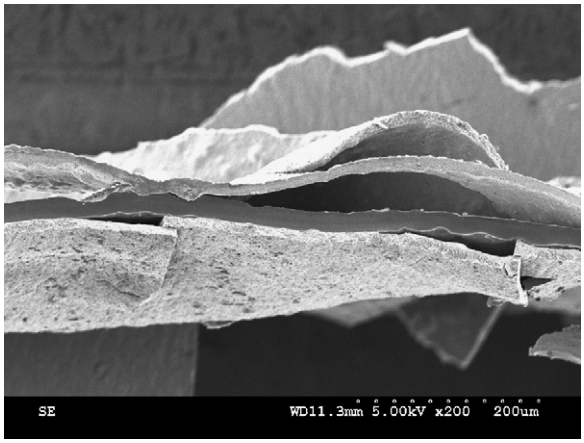

Fig. 13. Cross-sectional images of F/T cycled non-cracked CL with 18 μm non-reinforced membrane without DM located under the channel.

damage, and negligible damage under frozen conditions indicates that the DM/MPL combination can generally withstand F/T cycling.

Figs. 15 and 16 show surface and cross-sectional SEM images of a thermally cycled initially cracked CL with 18 μm reinforced membrane with DM/MPL. In this case, it is obvious that the initial cracks in CL promote severe damage. Compared to the non-cracked 18 μm case, the DM/MPL reduced the extent of F/T damage observed in Figs. 8 and 9, but CL delamination and frost heave were observed under the channels. Under the lands, there does appear to be some morphological change in the cracks, but no delamination was observed.

Figs. 17 and 18 show surface and cross-sectional SEM images of a thermally cycled initially non-cracked CL with 18 μm non-reinforced membrane with DM/MPL. As in the non-DM testing, with these samples, there was much more severe damage of the under-the-channel location of the frozen samples compared to the reinforced membrane results of the same thickness. The DM/MPL reduced significant surface damage because the DM/MPL can block liquid water contact in MEA as well as absorb stress due to ice expansion. However, it should be noted that DM/MPL cannot completely prevent interfacial delamination. A more dimensionally stable reinforced membrane [27] can help to limit the damage. Again, the non-frozen samples do not show any obvious morphological damage. Interestingly, there was no thin crack along the channel/land interface observed, as there had been for the case without DM.

Figs. 19 and 20 show surface and cross-sectional SEM images of a thermally cycled initially non-cracked CL with 35 μm reinforced membrane with DM/MPL. Fig. 21 shows additional SEM images of frost heave damage from under the channel locations of the same MEA type having undergone freeze cycling. The membrane in this case is reinforced, and protected by DM/MPL, and the virgin CL is non-cracked. However, the extensive frost heave damage and CL separation were observed compared to the similar 18 μm reinforced membrane case. This demonstrates conclusively that the membrane itself can be a source of water for damage in CL. As in all cases, the non-frozen thermally cycled samples do not show any obvious morphological damage, and severe delamination or surface heave of frozen cells is limited to under-the-channel locations.

4. Discussion

In summary, thermal cycling without freeze did not cause significant damage for all cases in the water immersion test conditions. However, line cracks along channel/land interfaces were observed for 35 μm reinforced membrane and 18 μm non-

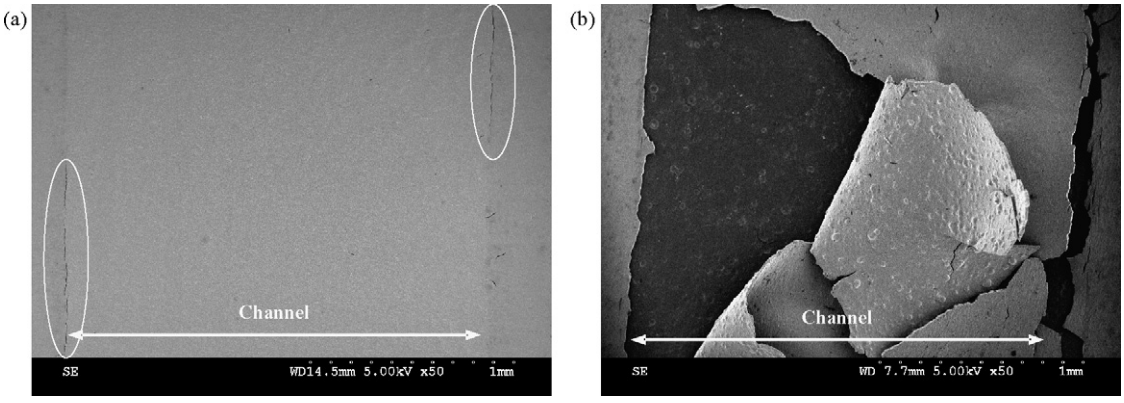

Fig. 12. SEM surface images of thermally cycled non-cracked CL with 18 μm non-reinforced membrane without DM located under the channel: (a) 5 °C/70 °C and (b) −40 °C/70 °C.

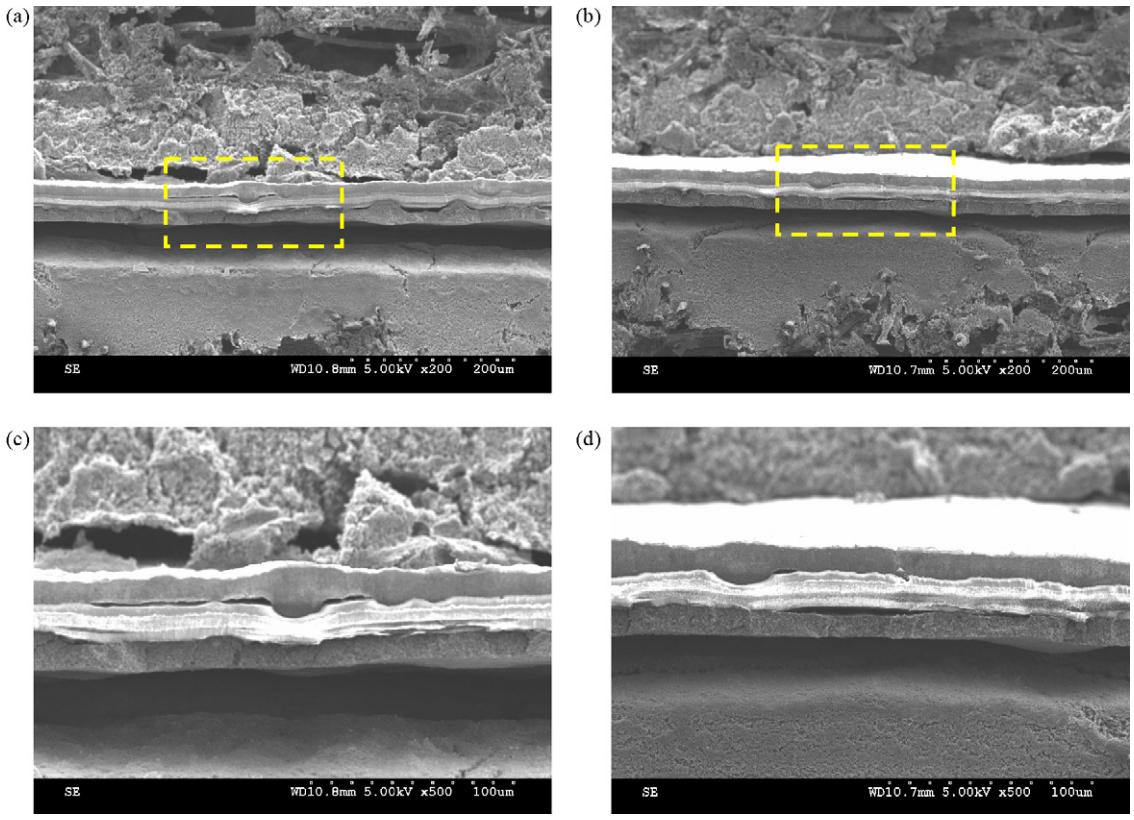

Fig. 14. Cross-sectional images of F/T cycled non-cracked CL with 18 μm reinforced membrane under the channel locations with DM/MPL: (c) and (d) are magnified images of the dotted box of (a) and (b), respectively.

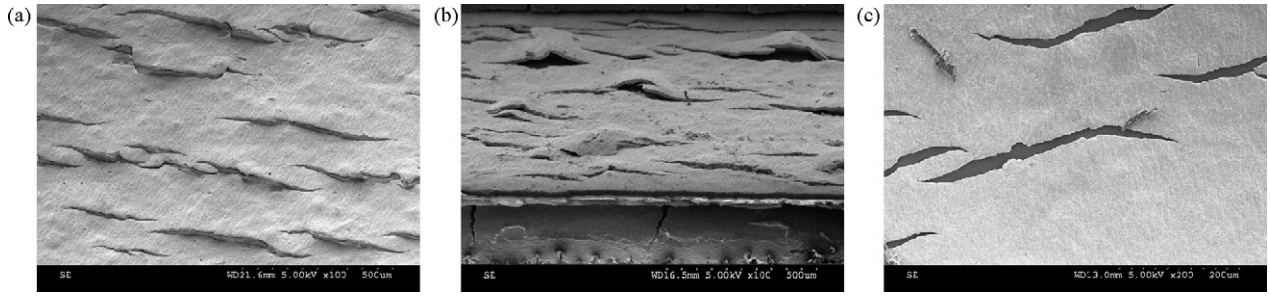

Fig. 15. SEM surface images of thermally cycled initially cracked CL with 18 μm reinforced membrane with DM/MPL: (a) land, −40 °C/70 °C, 100×, (b) channel, −40 °C/70 °C, 100× and (c) land, 5 °C/70 °C, 200×.

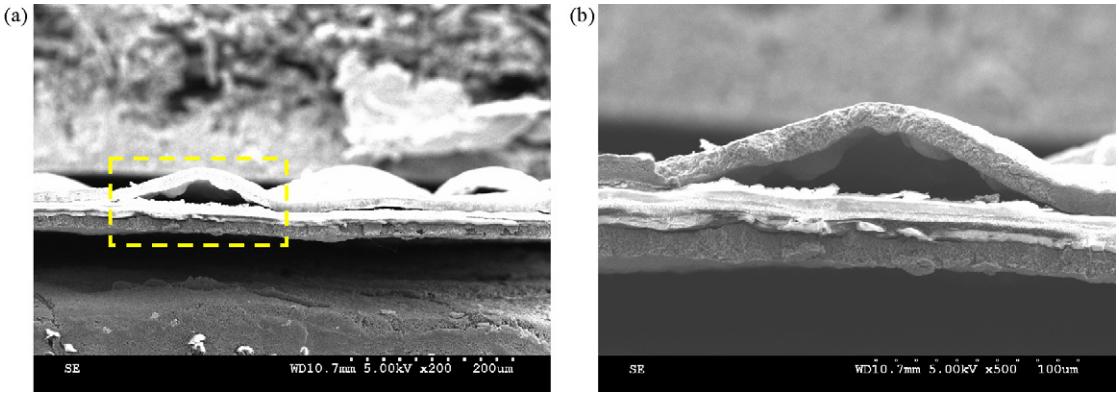

Fig. 16. SEM cross-sectional images of F/T cycled initially cracked CL with 18 μm reinforced membrane under the channel location with DM/MPL: (b) magnified image of the dotted box of (a).

Table 3
Summary of ex situ F/T cycling test of four different micro-structured MEAs under channels[a]

Thermal cycles	MEA type			
	Non-cracked CL with 18 μm reinforced membrane	Cracked CL with 18 μm reinforced membrane	Non-cracked CL with 35 μm reinforced membrane	Non-cracked CL with 18 μm non-reinforced membrane
70 °C/5 °C no DM/MPL	Negligible damage	Negligible damage	Negligible but line cracks along channel/land interface	Negligible but line cracks along channel/land interface
70 °C/−40 °C no DM/MPL	CL delamination	Severe CL damage and delamination	Severe CL damage and delamination	Severe CL damage and delamination
70 °C/5 °C with DM/MPL	Negligible damage	Negligible damage	Negligible damage	Negligible damage
70 °C/−40 °C (with DM/MPL)	Negligible damage	Slight surface damage, but severe interfacial separation and heave	Slight surface damage, but severe interfacial separation and heave	Slight surface damage, but severe interfacial separation and heave

[a] CL damage under lands was negligible for all cases.

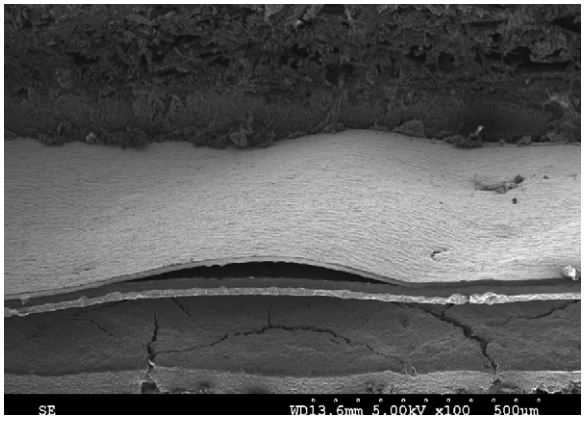

Fig. 17. SEM surface image of F/T cycled non-cracked CL with 18 μm non-reinforced membrane under the channel location with DM/MPL.

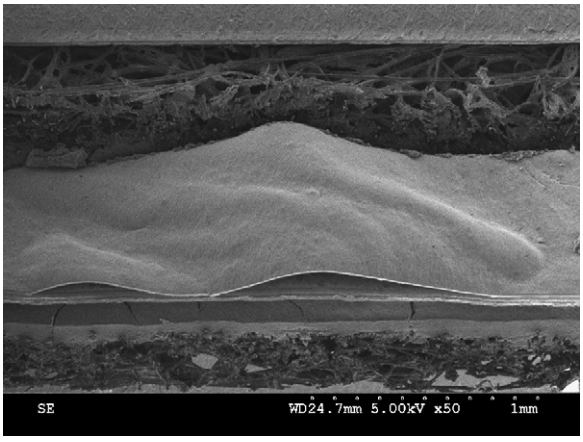

Fig. 19. SEM surface image of F/T cycled non-cracked CL with 35 μm reinforced membrane under the channel location with DM/MPL.

reinforced membrane cases, of which the damage was prevented using a rigid diffusion media (SGL10BB). Damage to the catalyst layers under lands was not observable for both freezing and non-freezing cases. Damage of catalysts layers under channels was strongly dependent upon micro-structures of MEAs and existence of a rigid gas diffusion layer with MPL. Rigid diffusion media reduces the surface damage of catalyst layers significantly, but could not prevent all interfacial delamination between membrane and catalyst layers observed. Interfacial delamination of CL from membrane and frost heave were observed for thicker (35 μm) membranes, cracked catalyst layers and non-reinforced membrane. However, non-cracked catalyst layers with thinner (18 μm) reinforced membrane showed negligible damage. It should also be noted that the membrane cracks or holes seen by other studies [12–14] were not observed for any cases. The test results are summarized in Table 3.

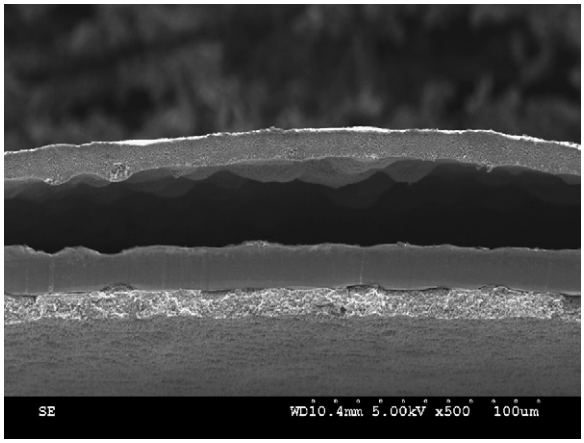

Fig. 18. Cross-sectional image of F/T cycled non-cracked CL with 18 μm non-reinforced membrane under the channel location with DM/MPL.

From SEM images of three different micro-structured MEAs with and without DM/MPL, the extent of damage was different, but interfacial delamination (membrane/catalyst layers) and frost heaves were common. F/T damage behaviors can be classified into two basic modes: (1) interfacial delamination by frost heave and (2) ice expansion damage. Damage of the catalyst layer of MEAs with DM/MPL was similar to frost heave damage in the road surfaces exposed under freezing conditions, as shown in Fig. 22(a) and (b). The schematic of frost heave damage mode proposed for PEFC [1,2] is depicted in Fig. 22(c). Liquid water transport rate, heat transfer, residual liquid water, and water phase in the fuel cell materials during the freezing are important factors for this damage mode. From comparison of SEM images of non-cracked MEAs with DM/MPL with 18 μm reinforced/non-reinforced and 35 μm reinforced mem-

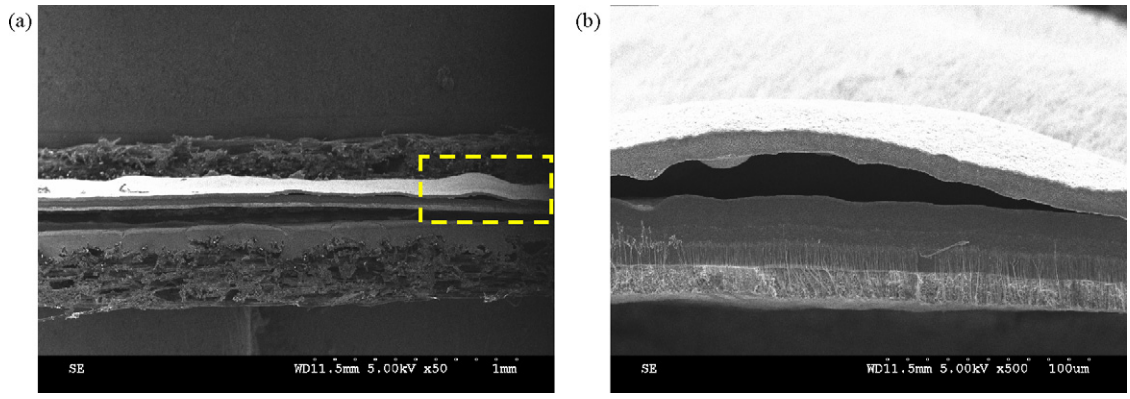

Fig. 20. Cross-sectional images of F/T cycled non-cracked CL with 35 μm reinforced membrane under the channel location with DM/MPL: (b) magnified image of the dotted box in (a).

branes (Figs. 14, 18 and 20), the damage is ascribed to the membrane itself because the only difference was the membrane thickness and reinforcement. The damage mode can be explained by considering factors of frost heave damage in the following ways.

As mentioned in Section 2, heat transfer rate may be a factor in F/T damage, but it is not a factor in this study. In this study, the water content in the ionomers inside CL and membrane was expected to have liquid equilibrated water content ($\lambda > 14$), as the MEAs were in direct contact with liquid water in these test conditions. Even if DM/MPL was used, the pressurized condition induced during the soaking step at 70 °C enabled liquid water to penetrate into the catalyst layers, because the pressure is higher than the measured breakthrough pressure of about 7 kPag for virgin SGL10BB DM. Thus liquid water saturation in DM was expected to be more 50%.

There are two water sources for ice lens growth. One is inside the MEA, and the other is outside the MEA in the pores of the CL and DM. The freezing point depression of diffusion media is negligible, and that of pores in the CL is less than 2 °C [23,24], but water freezing inside the membrane occurs from 0 °C to below −20 °C [4–6]. From the fact that non-cracked CL with 18 μm reinforced membrane experienced negligible F/T damage while the non-cracked CL with 35 μm reinforced membrane

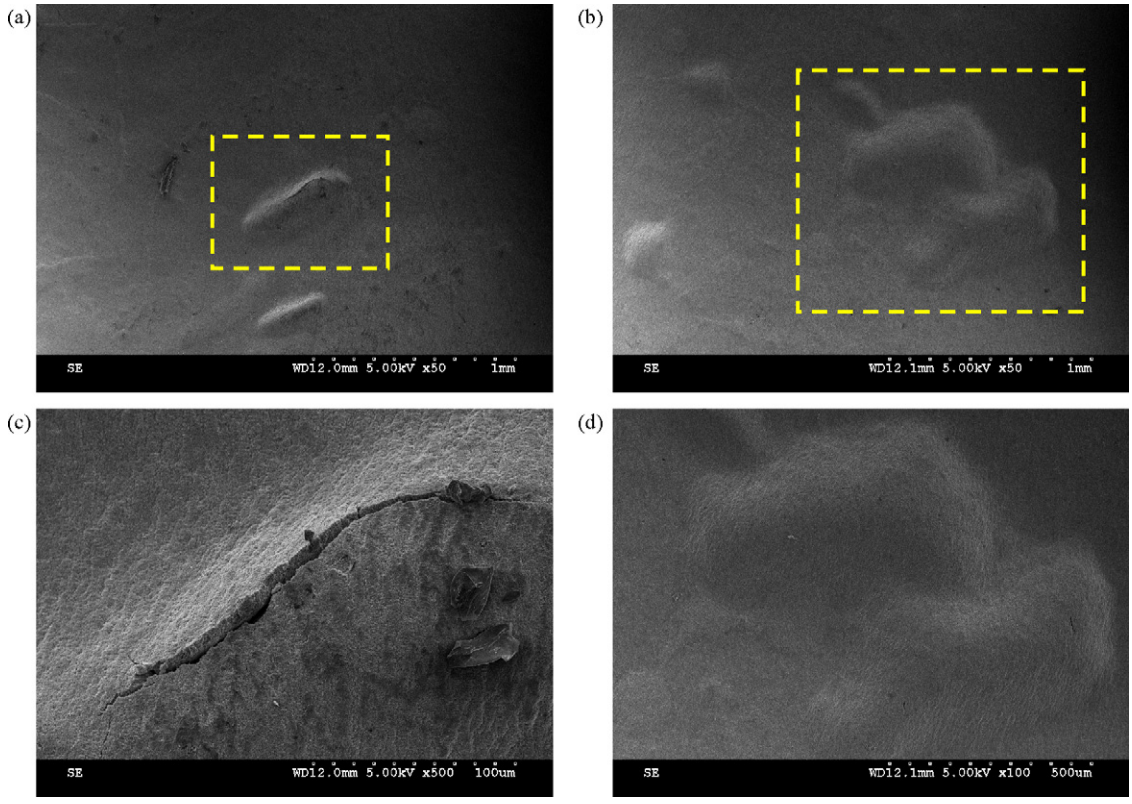

Fig. 21. Additional SEM surface images from under the channel of thermally frozen cycled (−40 °C to 70 °C) cycled non-cracked CL with 35 μm reinforced membrane with DM/MPL: (c) and (d) are magnified images of the dotted box in (a) and (b) each.

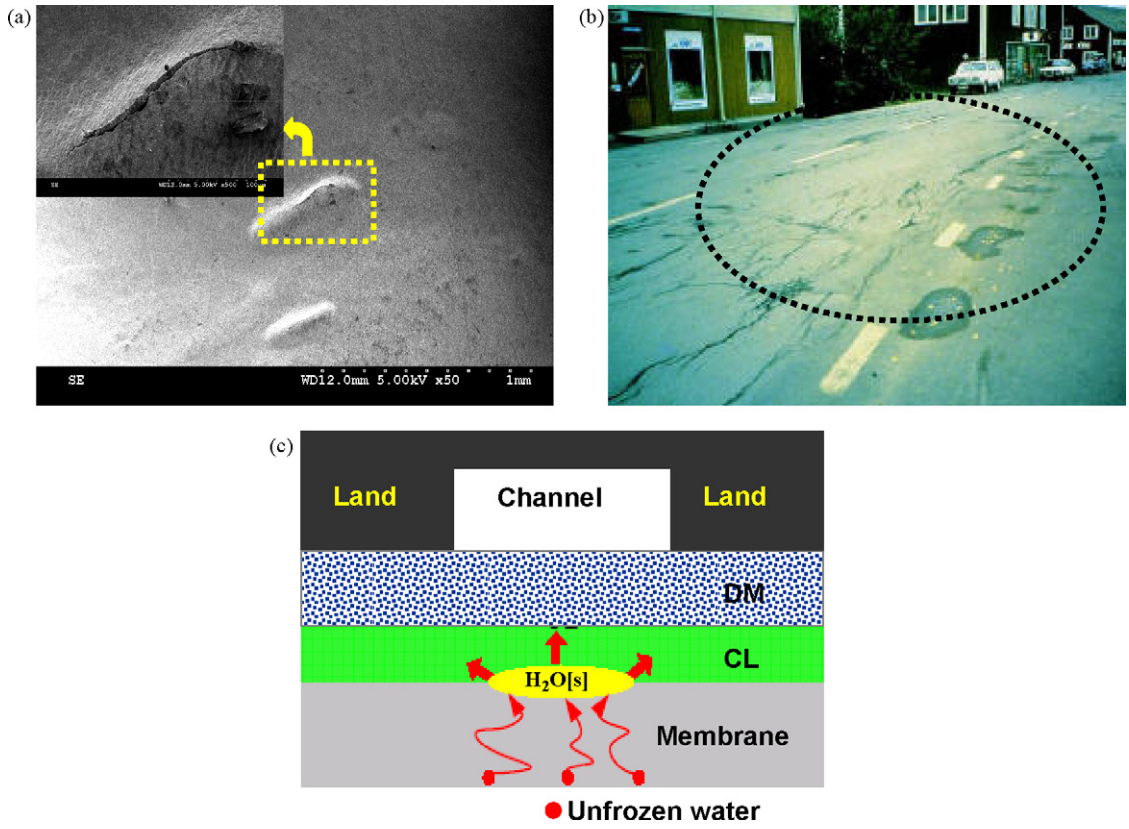

Fig. 22. Direct evidence of frost heave in PEFCs. (a) Heave and crack of a F/T cycled MEA, (b) frost heave on a city street in Sweden [28], and (c) schematic of frost heave damage mode.

experienced severe damage, the water inside the membrane was shown to be a source of water for frost heave interfacial delamination. The water outside the MEA (DM and channels) did not contribute to frost heave damage.

The water amount inside the membrane is determined by the ionomers and liquid contact. As freezing proceeds, the temperature of the membrane is the highest in the test cell. During the freezing, free water may be frozen inside the membrane or transported to the interface of membrane and CL, where liquid water is changed into ice. Loosely bounded water transports into the interface over a longer time scale compared to free water. The total water amount in thicker (35 μm) membrane is higher than that of thinner (18 μm) membrane. The water amount of non-reinforced membrane is also slightly higher than that of reinforced membrane due to the reinforcement structure. Therefore some liquid water contact with the ionomer on shutdown is a critical factor for damage to occur. Note that water content is different with direct liquid water contact or vapor equilibrated condition. Separate tests were performed with vapor-equilibrated sample, which did not show any observable damage. Due to the full submersion, more damage is expected in these test conditions. However, these conditions simulate localized sites of flow field of real fuel cells, when the liquid water is not fully purged during the shutdown.

Catalyst layers under the lands were not damaged in all test cases, but CLs under the channels were severely damaged. As predicted in the modeling work [1,2], CL/membrane interface delamination was not observed because ice lens under the land cannot grow due to lower ice lens pressure compared to the cell assembly pressure. These results imply that narrower channel width and stiffer diffusion media may be preferable to mitigate F/T damage. Ongoing work is clarifying the role of stiffness and compressive stress transmission on frost heave suppression and will be reported in a separate publication.

In addition to frost heave interfacial damage mode, ice expansion can cause F/T damage. From comparison of F/T damage of non-cracked and cracked catalyst layers with 18 μm reinforced membrane (Figs. 14 and 16), the F/T damage mechanism of the cracked catalyst layers may be different from that of the non-cracked MEAs, as depicted in Fig. 23. The crack gap (10–18 μm) is large enough to have negligible depression in the freezing point, so that liquid water in the crack gap is likely to behave like water inside the channel during the freezing. This liquid water is difficult to drain on shutdown in a fuel cell due to the MPL. For the case of a DM/MPL, the cracks in CL will be a location of relatively low capillary pressure. Therefore, MPL will offer no real protection in this submerged scenario, since any saturation in the MPL will drain into CL and be trapped until freezing occurs. Essentially, cracks in CL, when a highly hydrophobic media are involved, trap liquid water. If using a cracked electrode, it may be likely that a non-MPL coated DM would be preferred, since some water could more easily drain from these locations upon shutdown. To remove this trapped water, evaporation is needed. The interface between membrane and CL inside the crack can act as a crack initiation site and ice formation can exacerbate its growth because of shear stress induced by ice expansion inside

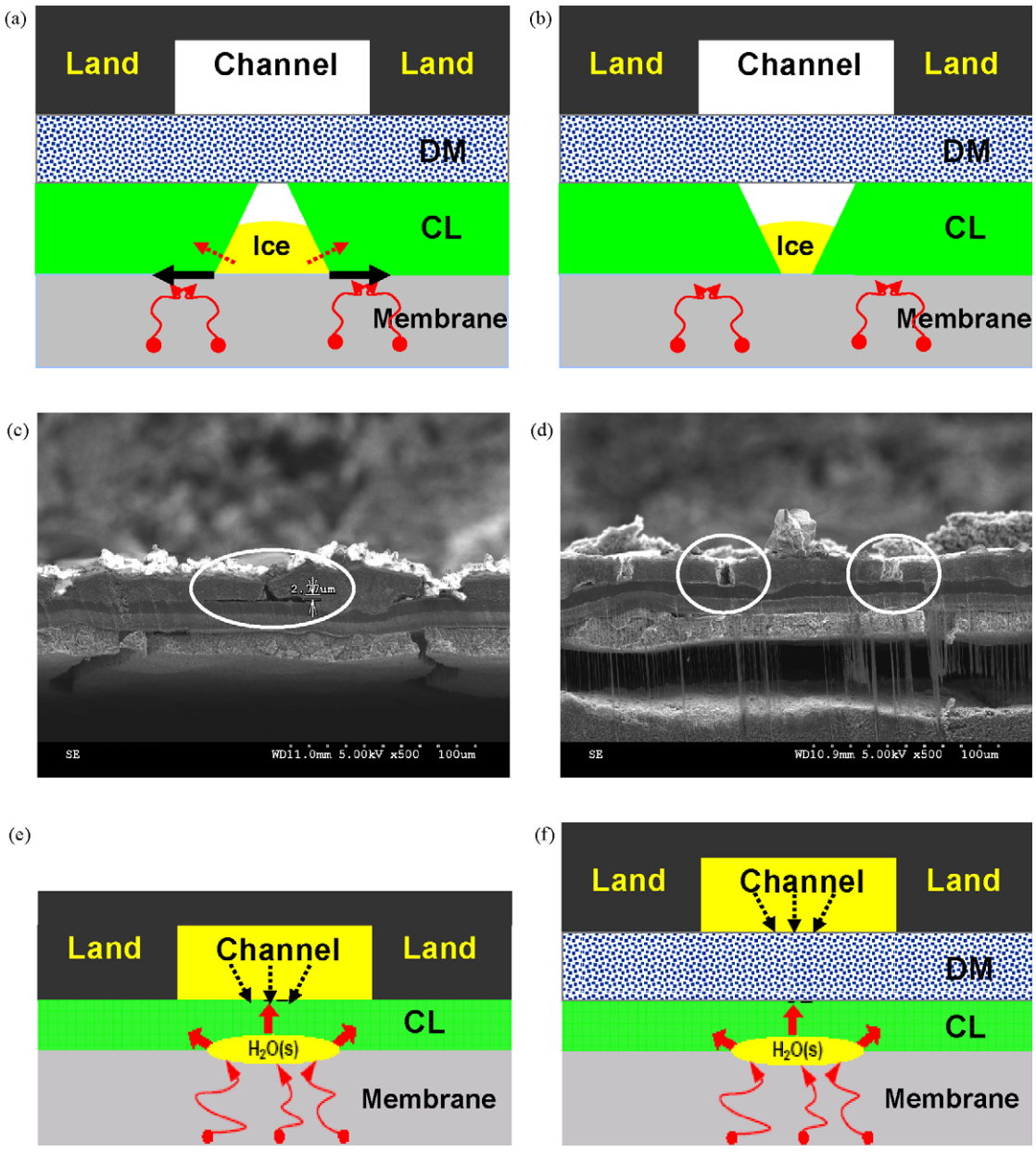

Fig. 23. Schematic of possible ice expansion damage modes. (a) Inverted V-shaped cracked MEA, (b) V-shaped cracked MEA, (c) and (d) evidences of inverted V-shaped crack shapes, (e) non-cracked MEA without DM/MPL, and (f) non-cracked MEA with DM/MPL.

the crack, especially in the inverted V-shaped cracks as shown in Fig. 23(a). However, the upward V-shaped crack may not affect crack growth because stress induced by ice expansion would not contribute to crack initiation along the interface, as shown in Fig. 23(b). As shown in the cross-sectional view of the virgin cracked 18 μm MEA of Fig. 23(c) and (d), the bottom gap of the crack was slightly larger than the surface gap. Therefore, we can conclude that the damage of the cracked MEAs during the F/T cycling was greater than the non-cracked MEA because of local water pooling and ice expansion stress.

Catalyst layers without DM/MPL were much more severely damaged compared to those with DM/MPL cases. For the non-cracked CL with 18 μm reinforced membrane (Figs. 7 and 14), interfacial delamination was observed without a DM/MPL, but was negligible with a DM/MPL. All MEAs showed significantly reduced damage using a DM/MPL, but interfacial delamination and heave damage could not be completely prevented. There may be another potential pore level damage in the catalyst layer by ice expansion. This pore level damage cannot be observed by SEM, but can be studied by investigating pore size distribution using mercury intrusion or other methods.

Ice expansion in the confined channels can cause stress if the expanded volume cannot be absorbed by porous media. Ice formation may have occurred first in the lower and top of the vertical channels, blocking water flow through the channel, and causing stress on CL, resulting in bending or fracture of CL, as shown in Fig. 23(e). As shown in Fig. 23(f), the DM/MPL can serve as mechanical buffer layers to absorb stress, and can restrict direct contact of liquid water, mitigating this damage.

As shown in the thermal cycling without freezing, line cracks along the channel/land interfaces observed in thicker membrane and non-reinforced membrane were attributed to greater swelling. Increased swelling exacerbates interfacial delamination between membrane and catalyst layers and can accelerate both F/T damage modes (frost heave and ice expansion). The mechanisms for this occurrence can be ionomer expansion of frozen water inside the membrane, or ice lens formation, but nevertheless the membrane is a source of damage. The thinner the membrane, the less the water, and therefore the less damage is expected.

It is difficult to quantify the relative level of importance with the testing done here, but clearly the diffusion media (either through the stiffness or highly hydrophobic MPL), the thickness, the reinforcement, and the initial surface cracks all play an important role in frost heave damage. It should be noted that the damage from the membrane itself can likely be eliminated with a purge of the system on shutdown to remove residual liquid water in contact with the electrolyte. Reduction of the liquid contact with the membrane on shutdown by natural drainage processes (non-parasitic effects) is a focus of continued study.

5. Conclusions

This extensive investigation of ex situ MEAs and DM/MPL testing has revealed very strong direction for the material choices in the PEFC and helped to conceptually validate the previous computational model performed of Mench and coworkers [1,2]. Specifically, the membrane was found to be a source of water that can damage the MEA upon thermal cycling to $-40\,^{\circ}C$. Damage was found to occur almost exclusively under the channel, except for an along the land interface line crack that develops for non-DM equipped samples immersed in liquid. From the fact that there was no damage under the land in the worst scenario of direct liquid contact with no diffusion media, the channel to land ratio are also important factors in damage mitigation. Although the larger land can be better for F/T, at a certain point it would cause dead zones in the center of land and worsen flooding in high RH conditions. The preferred material to reduce F/T damage is a crack free catalyst layer with low water content and dimensionally stable membrane, with a stiff diffusion media. The role of the DM is not yet fully understood. It helps to provide a stiff boundary to prevent expansion and eliminating interfacial gaps which can serve as and a pooling location, and as a hydrophobic barrier to limit water intrusion. However, it can also detrimentally trap residual liquid water in the catalyst layer on shutdown. In order to prevent F/T damage, it is necessary that the liquid contact with the membrane is reduced or eliminated, which can be accomplished through a variety of parasitic and non-parasitic approaches beyond the scope of this work.

Acknowledgements

This research was supported by the Advanced Technology Center, R&D Division for Hyundai Motor Company. The authors are grateful to W.L. Gore and Associates for supplying MEA samples and to Dr. S. Cleghorn and Mr. M. Crum for helpful discussions and insight. The authors are also appreciative of Mr. K. Heller's help to analyze crack density and Dr. E.C. Kumbur's measurement of breakthrough pressure.

References

[1] S. He, M.M. Mench, J. Electrochem. Soc. 153 (2006) A1724–A1731.
[2] S. He, S.H. Kim, M.M. Mench, J. Electrochem. Soc. 154 (2007) B1024–B1033.
[3] US Department of Energy, Hydrogen Fuel Cells and Infrastructure Technologies Program, 2005. www.eere.energy.gov/hydrogenandfuelcells/mypp/pdfs/fuel_cells.pdf.
[4] Y.S. Kim, L. Dong, M.A. Hickner, T.E. Glass, V. Webb, J.E. McGrath, Macromolecules 36 (2003) 6291–6295.
[5] M. Saito, N. Arimura, K. Hayamizu, T. Okada, J. Phys. Chem. B 109 (2005) 3112–3119.
[6] A. Siu, J. Schmeisser, S. Holdcroft, J. Phys. Chem. B 110 (2006) 6072–6080.
[7] R.C. McDonald, C.K. Mittelsteadt, E.L. Thompson, Fuel Cells 4 (2004) 208–213.
[8] Q. Guo, Z. Qi, J. Power Sources 160 (2006) 1269–1274.
[9] J. Hou, H. Yu, S. Zhang, S. Sun, H. Wang, B. Yi, P. Ming, J. Power Sources 162 (2006) 513–520.
[10] E.A. Cho, J.J. Ko, H.Y. Ha, S.A. Hong, K.Y. Lee, T.W. Lim, I.H. Oh, J. Electrochem. Soc. 151 (2004) A661–A665.
[11] E.A. Cho, J.J. Ko, H.Y. Ha, S.A. Hong, K.Y. Lee, T.W. Lim, I.H. Oh, J. Electrochem. Soc. 150 (2003) A1667–A1670.
[12] R. Gaylord, Stationary application and freeze/thaw, Presented at US Department of Energy, Workshop on Fuel Cell Operations at Sub-Freezing Temperatures, Washington DC, 2005.
[13] J.P. Meyers, Fundamental issues in subzero PEMFC startup and operation, Presented at US Department of Energy, Workshop on Fuel Cell Operations at Sub-Freezing Temperatures, Washington DC, 2005.
[14] Q. Yan, H. Toghiani, Y. Lee, K. Liang, H. Causey, J. Power Sources 160 (2006) 1242–1250.
[15] M.S. Wilson, J.A. Valerio, S. Gottesfeld, Electrochim. Acta 40 (1995) 355–363.
[16] R. Mukundan, Y.S. Kim, F. Garzon, B. Pivovar, ECS Trans. 1 (2006) 403–413.
[17] R. Mukundan, Y.S. Kim, F. Garzon, B. Pivovar, DOE Hydrogen Program Annual Progress Report, 2006, pp. 926–929.
[18] H. Liu, Dimensionally stable high performance membrane, Presented at US Department of Energy, Hydrogen Program Annual Merit Review Workshop, Washington DC, 2006.
[19] T. Patterson, R. Balliet, DOE Hydrogen Program Annual Progress Report, 2006, pp. 910–912.
[20] T. Patterson and J.P. Meyers, PEM fuel cell freeze durability and cold start project, Presented at US Department of Energy, Hydrogen Program Annual Merit Review Workshop, Washington DC, 2006.
[21] M. Oszcipok, D. Riemann, U. Kronenwett, M. Kreideweis, M. Zedda, J. Power Sources 145 (2005) 407–515.
[22] M. Oszcipok, M. Zedda, D. Riemann, D. Geckeler, J. Power Sources 154 (2006) 404–411.
[23] S. Ge, C.Y. Wang, Electrochem. Solid State Lett. 9 (2006) A499–A503.
[24] S. Ge, C.Y. Wang, Electrochim. Acta 52 (2007) 4825–4835.
[25] E.C. Kumbur, K.V. Sharp, M.M. Mench, J. Electrochem. Soc., in press.
[26] http://rsb.info.nih.gov/ij/.
[27] S. Cleghorn, J. Kolde, W. Liu, in: W. Vielstich, H.A. Gasteiger, A. Lamm (Eds.), Handbook of Fuel Cells, Fundamentals, Technology and Applications, 566, John Wiley & Sons, New York, 2003.
[28] http://training.ce.washington.edu/WSDOT/Modules/04_design_parameters/04-4_body.htm#thaw_weakening.